Statistical evaluation of the B-Splines approximation of 3D point clouds

Hamza ALKHATIB, Boris KARGOLL, Johannes BUREICK, Jens-André PAFFENHOLZ, Germany

Key words: terrestrial laser scanning, 3D point cloud, B-Splines, deformation analysis, monitoring, statistical model selection

SUMMARY

Terrestrial laser scanning (TLS) has proved to be a suitable technique for geodetic monitoring of infrastructure buildings such as bridges as it allows to determine object changes and deformations rapidly with high precision as well as high spatio-temporal resolution. In addition, this monitoring includes the evaluation of their life cycle and the developing of concepts to increase their expected life time. In an interdisciplinary project, which is being conducted with partners from industry and research, an historic masonry arch bridge over the river Aller near Verden (Lower Saxony, Germany) has been investigated. Besides different other sensors, a terrestrial laser scanner was used to measure the vertical deflection of the bridge construction under different load scenarios. The resulting 3D point clouds have been spatially approximated using approaches of free-form curves and surfaces, based on B-Splines. The selection of the degree of the basis functions and of the number of control points has a considerable and crucial effect on the estimating results of the B-Splines. To assess the statistical significance of the differences displayed by the estimates for different model choices, two non-nested model selection tests as well as information criteria will be adopted and applied.

Statistical Evaluation of the B-Splines Approximation of 3D Point Clouds (9634)
Hamza Alkhatib, Boris Kargoll, Jens-André Paffenholz and Johannes Bureick (Germany)

FIG Congress 2018
Embracing our smart world where the continents connect: enhancing the geospatial maturity of societies
Istanbul, Turkey, May 6–11, 2018

Statistical evaluation of the B-Splines approximation of 3D point clouds

Hamza ALKHATIB, Boris KARGOLL, Johannes BUREICK, Jens-André PAFFENHOLZ, Germany

1. INTRODUCTION

Free-form curves and surfaces have been used as part of a standard approximation method for point clouds in many engineering disciplines in the past decade. The point clouds are captured, e.g., by TLS, which has been found to be a useful observation technique in different geodetic applications such as 3D surface modeling, monitoring and deformation analysis. For example, Koch (2009), Harmening & Neuner (2015), and Bureick et al. (2016) modeled the captured point clouds by means of B-Splines and Non-uniform rational B-Splines (NURBS). In addition, Bureick et al. (2016) and Xu et al. (2017) used B-Splines for the monitoring of different structures, such as rails and arches. However, the determination of the knots in B-Spline approximation (known as knot adjustment problem) affects the estimation of the curve and surface significantly. Therefore, in Bureick et al. (2016) and Bureick & Alkhatib (2018) different approaches based on Monte Carlo techniques and genetic algorithms are developed. Both approaches show an optimal selection and optimization of knot vectors for curve approximation.

The second important issue for an optimal B-Spline approximation is the adequate number of control points, known as model selection. In case of B-Spline surfaces, model selection comprises a suitable choice of the degree of the basis functions as well as the number of control points in two different directions. In many cases this task is solved by applying an information criterion, like the Akaike information criterion (AIC) or the Bayesian information criterion (BIC). Harmening & Neuner (2016) applied structural risk minimization, originating from statistical learning theory to determine the optimal degree and number of control points of B-spline curves. In Harmening & Neuner (2017) this approach is extended to B-spline surfaces. In this paper we apply two non-nested model selection tests, which are based on an information criterion: the Vuong's testing (Vuong,1989) and the Clarke's testing approach (see, e.g., Clarke, 2007). Two models are non-nested or separate if one model cannot be obtained as limit of the other (or one model is not a particular case of the other). The Vuong test has been widely used in non-nested model selection under the normality assumption. While the Vuong test determines whether the average log-likelihood ratio is statistically different from zero, the distribution-free test proposed by Clarke determines whether or not the median log-likelihood ratio is statistically different from zero. Two B-Spline models with different degrees or control points ("model I" and "model II") are non-nested because the parameters in model I are not a subset of the parameters in model II. The modification of the degree or the number of control points leads to changing the number of knots, resulting in different basis functions. Zhao et al. (2018) applied Voung's hypothesis tests for model selection in B-Spline surface approximation.

Statistical Evaluation of the B-Splines Approximation of 3D Point Clouds (9634)
Hamza Alkhatib, Boris Kargoll, Jens-André Paffenholz and Johannes Bureick (Germany)

FIG Congress 2018
Embracing our smart world where the continents connect: enhancing the geospatial maturity of societies
Istanbul, Turkey, May 6–11, 2018

This paper focuses on the optimal selection of the most parsimonious, yet sufficiently accurate, parametric description of a structure based on TLS measurements by changing the number of control points and by selecting the optimal approach for the determination of the knot vectors.

2. MATHEMATICAL BASICS

2.1 B-Spline surfaces

A 3D point $\boldsymbol{S}(\bar{u}, \bar{v})$ lying on a B-Spline surface is defined by:

$$\boldsymbol{S}(\bar{u}, \bar{v}) = [x(\bar{u}, \bar{v}), y(\bar{u}, \bar{v}), z(\bar{u}, \bar{v})]^T = \sum_{i=0}^{n} \sum_{j=0}^{l} N_{i,p}(\bar{u}) N_{j,q}(\bar{v}) \boldsymbol{x}_{i,j} \text{ with } \boldsymbol{x}_{i,j}$$

$$= [x_{i,j}, y_{i,j}, z_{i,j}].$$

Eq. 1

$\boldsymbol{S}(\bar{u}, \bar{v})$ is calculated by the totalised linear combinations of the basis functions $N_{i,p}(\bar{u}), N_{j,q}(\bar{v})$ and the control point array $\boldsymbol{x}_{i,j}$. Altogether $(n+1) \times (l+1)$ linear combinations and therefore the same amount of control points and basis functions contribute to $\boldsymbol{S}(\bar{u}, \bar{v})$. The position of $\boldsymbol{S}(\bar{u}, \bar{v})$ on the B-Spline surface is defined by the location parameters $\bar{u}$ and $\bar{v}$. $\bar{u}$ is the location parameter in the first direction ($\bar{u}$-direction) and $\bar{v}$ is the location parameter in the direction perpendicular to the $\bar{u}$-direction ($\bar{v}$-direction). The degrees of the basis functions in $\bar{u}$-direction and $\bar{v}$-direction are defined by p and q, respectively. In $\bar{u}$-direction the basis functions $N_{i,p}(\bar{u})$ depend on $\bar{u}, p$ and the, so called, knot vector $\mathbf{U}$. $\mathbf{U}$ consists of $m+1$ (with $m = n + p + 1$) knots, which are arranged in a non-decreasing order:

$$\mathbf{U} = [u_0, \dots, u_m] \text{ with } u_i \leq u_{i+1}, i \in \{0, \dots, m-1\}.$$

Eq. 2

In $\bar{v}$-direction the basis functions $N_{j,q}(\bar{v})$ depend on $\bar{v}, q$ and the knot vector $\mathbf{V}$. $\mathbf{V}$ consists of $r + 1$ (with $r = l + q + 1$) knots, which are also arranged in a non-decreasing order.

Cox (1972) and de Boor (1972) developed a recursive function to calculate the basis functions. For $N_{i,p}(\bar{u})$ the recursive function reads as follows:

$$N_{i,0}(\bar{u}) = \begin{cases} 1 \text{ if } u_i \leq \bar{u} \leq u_{i+1}, \\ 0 \text{ otherwise.} \end{cases}$$

$$N_{i,p}(\bar{u}) = \frac{\bar{u} - u_i}{u_{i+p} - u_i} N_{i,p-1}(\bar{u}) + \frac{u_{i+p+1} - \bar{u}}{u_{i+p+1} - u_{i+1}} N_{i+1,p-1}(\bar{u}).$$

Eq. 3

$N_{j,q}(\bar{v})$ is calculated analogously.

When a B-Spline surface is applied to approximate a 3D point cloud, beside model selection (see Sec. 2.2) usually the 3 main steps:

- parametrisation (Sec. 2.1.1),
- knot vector determination (Sec. 2.1.2) and
- control point estimation (Sec. 2.1.3)

have to be accomplished.

Statistical Evaluation of the B-Splines Approximation of 3D Point Clouds (9634)
Hamza Alkhatib, Boris Kargoll, Jens-André Paffenholz and Johannes Bureick (Germany)

FIG Congress 2018
Embracing our smart world where the continents connect: enhancing the geospatial maturity of societies
Istanbul, Turkey, May 6–11, 2018

2.1.1 Parametrization

Parametrization comprises the determination of location parameters $\bar{u}$ and $\bar{v}$ for each point in the 3D point cloud. In case of an irregularly shaped point cloud this task may become quite tricky and sophisticated methods have to be applied (see for instance Harmening & Neuner (2015), Ma & Kruth (1995)). Since we analyse a regularly and rectangularly shaped point cloud, we use the simple technique described in Piegl & Tiller (1997). The point cloud represents a rectangular grid with s rows and t columns. For each row, the t location parameters $\bar{u}_1^i$ to $\bar{u}_t^i$ (with $i = 1, \ldots, s$) are calculated using the chord length method, mentioned in Piegl & Tiller (1997). In this method the Euclidean distance between adjacent points is calculated. The totalised Euclidean distance so far is assigned to each point. At the end this value is normalized by a division through the totalised Euclidean distance assigned to the last point of the row. The average of the s realisations of $\bar{u}_1^i$ to $\bar{u}_t^i$ represents the parametrisation in $\bar{u}$-direction:

$$\bar{u}_k = \frac{1}{s}\sum_{i=1}^{s} \bar{u}_k^i \text{ with } k = 1, \ldots, t. \qquad \text{Eq. 4}$$

The calculation of the parametrisation in $\bar{v}$-direction proceeds in an analogous manner.

2.1.2 Knot vector determination

An important step in B-Spline surface approximation is the determination of suitable knot vectors **U** and **V**. This so called knot adjustment problem is known to be a multimodal, multivariate continuous nonlinear optimisation problem (see for instance Dierckx (1993), Gálvez et al. (2015), Bureick & Alkhatib (2018)). Due to a lack of an analytic expression for optimal knot locations, plenty of methodologies have been developed to solve the knot adjustment problem. For most of the methodologies the capability was shown for B-Spline curve approximation. The extension to B-Spline surfaces is often neglected, but assumed to be straightforward. In this paper we selected 2 methods and applied respectively extended them to B-Spline surfaces. The first method is the "knot placement technique"(KPT) described in Piegl & Tiller (1997, p. 412), which ensures that in each knot span at least one location parameter is placed. This leads to well conditioned matrices in the subsequent control point estimation. In $\bar{u}$-direction this method reads as follows:

$$
\begin{aligned}
d &= \frac{t}{n - p + 1} \\
i &= \text{int}(jd) \\
\alpha &= jd - i \\
u_{p+j} &= (1 - \alpha)\bar{u}_{i-1} + \alpha\bar{u}_i \text{ with } j = 1, \ldots, n - p
\end{aligned}
\qquad \text{Eq. 5}
$$

The second method we applied, is the Evolutionary Monte Carlo Method (MCM) described in Bureick et al. (2016) and Bureick & Alkhatib (2018). In this method random knot vectors are generated iteratively and applied on the point cloud to be approximated. The knot vectors which yield the best results are stored in a population. After some iterations this population is used to calculate a probability. The subsequent knot vectors are randomly chosen from this probability.

Statistical Evaluation of the B-Splines Approximation of 3D Point Clouds (9634)
Hamza Alkhatib, Boris Kargoll, Jens-André Paffenholz and Johannes Bureick (Germany)

FIG Congress 2018
Embracing our smart world where the continents connect: enhancing the geospatial maturity of societies
Istanbul, Turkey, May 6–11, 2018

On the one the meta-heuristic approach MCM yields significantly better results than the KPT. On the other hand the computational costs of MCM are much higher.

2.1.3 Control point estimation

The final step in the approximation process is the control point estimation. When the previous steps of parametrization and knot vector determination are accomplished, the unknown control points are optimally estimated in a Gauss-Markov model (GMM):

$$\mathbf{l} = \mathbf{Ax} + \boldsymbol{\varepsilon}. \qquad \text{Eq. 6}$$

The design matrix $\mathbf{A}$ is a block diagonal matrix consisting of the identical matrices $\mathbf{A}_x$, $\mathbf{A}_y$ and $\mathbf{A}_z$:

$$\mathbf{A}_x = \mathbf{A}_y = \mathbf{A}_z = \begin{bmatrix} N_{0,p}(\bar{u}_1)N_{0,q}(\bar{v}_1) & \cdots & N_{n,p}(\bar{u}_1)N_{l,q}(\bar{v}_1) \\ \vdots & \ddots & \vdots \\ N_{0,p}(\bar{u}_t)N_{0,q}(\bar{v}_s) & \cdots & N_{n,p}(\bar{u}_t)N_{l,q}(\bar{v}_s) \end{bmatrix}$$

$$\mathbf{A} = \begin{bmatrix} \mathbf{A}_x & \mathbf{0} & \mathbf{0} \\ \mathbf{0} & \mathbf{A}_y & \mathbf{0} \\ \mathbf{0} & \mathbf{0} & \mathbf{A}_z \end{bmatrix} \qquad \text{Eq. 7}$$

The observation vector is set up by the point cloud to be approximated:

$$\mathbf{l} = [Q_{x,1} \quad \cdots \quad Q_{x,s\times t} \quad Q_{y,1} \quad \cdots \quad Q_{y,s\times t} \quad Q_{z,1} \quad \cdots \quad Q_{z,s\times t}]^T. \qquad \text{Eq. 8}$$

The control points are estimated in a least square sense by minimizing the errors $\boldsymbol{\varepsilon}$:

$$\hat{\mathbf{x}} = [x_{0,0} \quad \cdots \quad x_{n,l} \quad y_{0,0} \quad \cdots \quad y_{n,l} \quad z_{0,0} \quad \cdots \quad z_{n,l}]^T = (\mathbf{A}^T\mathbf{PA})^{-1}\mathbf{A}^T\mathbf{Pl}. \qquad \text{Eq. 9}$$

$\mathbf{P}$ represents the weight matrix of the coordinate components of the point cloud. In the case of identical and independent normally distributed errors $\boldsymbol{\varepsilon}$, $\mathbf{P}$ is given by the identity matrix $\mathbf{I}$.

2.2 Model Selection

The Kullback-Leibler Information is a fundamental measure of distance of a fully specified probability density function (pdf) to another one (cf. Burnham & Anderson, 2002; Section 2.1). Since the pdf of certain observables usually involves unknown parameters to be estimated from the data in the course of an adjustment, several attempts have been made to use the Kullback-Leibler Information to derive a statistic (i.e., data-dependent quantity) that allow one either to measure the distance of the adjusted model to the true model or to test competing models against each other. In the remainder of this section, we summarize two well-known information criteria as well as two hypothesis tests (which apparently have not been applied to geodetic model selection problems, yet). The choice of these procedures is motivated by the fact that the competing models of our subsequent case study in Section 3 are *non-nested* in the sense that none of the (B-Spline) models is a special case of the other one. More specifically, under the usual assumption of normally distributed and homoskedastic observations (having common variance σ^2), the GMM in (6) translates into the logarithmized pdf or log-likelihood function

Statistical Evaluation of the B-Splines Approximation of 3D Point Clouds (9634)
Hamza Alkhatib, Boris Kargoll, Jens-André Paffenholz and Johannes Bureick (Germany)

FIG Congress 2018
Embracing our smart world where the continents connect: enhancing the geospatial maturity of societies
Istanbul, Turkey, May 6–11, 2018

$$L(\mathbf{x}, \sigma^2; \mathbf{l}) = \log \prod_{i=1}^{3 \cdot s \cdot t} \frac{1}{\sqrt{2\pi\sigma^2}} \exp\left\{-\frac{1}{2}\left(\frac{\mathbf{A}_i\mathbf{x} - l_i}{\sigma}\right)^2\right\} = \sum_{i=1}^{3 \cdot s \cdot t} L(\mathbf{x}, \sigma^2; l_i) \qquad \text{Eq. 10}$$

where the $3 \cdot s \cdot t$ rows $\mathbf{A}_i$ of the total design matrix $\mathbf{A}$ (corresponding to the $3 \cdot s \cdot t$ given measurements l_i in the total observation vector $\mathbf{l}$) depend on the specific parameterization of the B-spline model. Strictly speaking, the components of a B-Spline design matrix depend on the given measurements and constitute therefore random variables. However, to obtain a tractable testing problem, we condition the log-likelihood function on the given measurements and assume accordingly the components of the design matrix to be constants.

As a first step towards model selection testing, we apply the definitions of Akaike's Information Criterion

$$\text{AIC} = -2 \cdot L(\hat{\mathbf{x}}, \hat{\sigma}^2; \mathbf{l}) + 2 \cdot (3 \cdot [n+1] \cdot [l+1] + 1) \qquad \text{Eq. 11}$$

and of the Bayesian (sometimes also called Schwarz's) Information Criterion

$$\text{BIC} = -2 \cdot L(\hat{\mathbf{x}}, \hat{\sigma}^2; \mathbf{l}) + (3 \cdot [n+1] \cdot [l+1] + 1) \cdot \log(3 \cdot s \cdot t) \qquad \text{Eq. 12}$$

where the total number $3 \cdot [n+1] \cdot [l+1] + 1$ of estimated parameters is determined by the number $[n+1] \cdot [l+1]$ of control points, as well as by the single estimated variance. Notice that the least-squares estimate $\hat{\mathbf{x}}$ in (9) coincides with the maximum-likelihood (ML) estimates, whereas the least-squares estimate for the variance closely approximates the ML estimate $\hat{\sigma}^2$ when the redundancy is large (cf. Koch, 1999). When these information criteria are evaluated for different models/design matrices, the model with the smallest value gets selected. Since we will be interested in rigorously judging whether the selected model is *significantly* better than the other candidate models, we review now two extensions of AIC and BIC to statistical hypothesis tests.

2.2.1 Voung's Testing Approach

Instead of comparing the values that an information criterion takes at different models, Vuong's test compares two competing (adjusted) models via a test statistic, which exceeds critical values in cases of significant model differences. Under the null hypothesis, the two compared models are equivalent, i.e., there is no significant difference between them. Letting $\mathbf{A}^{(0)}\mathbf{x}^{(0)}$ and $\mathbf{A}^{(1)}\mathbf{x}^{(1)}$ represent two competing B-Spline models involving, for instance, different basis function degrees or different numbers of control points, the idea is to check whether the ML estimates $\hat{\mathbf{x}}^{(0)}, \hat{\sigma}^{(0)}$ and $\hat{\mathbf{x}}^{(1)}, \hat{\sigma}^{(1)}$ cause a very small or large difference $L(\hat{\mathbf{x}}^{(0)}, \hat{\sigma}^{2(0)}; \mathbf{l}) - L(\hat{\mathbf{x}}^{(1)}, \hat{\sigma}^{2(1)}; \mathbf{l})$ between the associated log-likelihoods. To do this, Vuong normalized this difference with $\hat{\omega}$ times the square root of the total number of observations (cf. Clarke, 2007; Section 2.1), which reads in our B-Spline selection problem

$$\hat{\omega} \cdot \sqrt{3 \cdot s \cdot t} = \sqrt{E - F} \cdot \sqrt{3 \cdot s \cdot t} \qquad \text{Eq. 13}$$

with

$$E = \frac{1}{3 \cdot s \cdot t} \sum_{i=1}^{3 \cdot s \cdot t} \left[L(\hat{\mathbf{x}}^{(0)}, \hat{\sigma}^{2(0)}; l_i) - L(\hat{\mathbf{x}}^{(1)}, \hat{\sigma}^{2(1)}; l_i)\right]^2 \qquad \text{Eq. 14}$$

and

$$F = \left[\frac{1}{3 \cdot s \cdot t} \sum_{i=1}^{3 \cdot s \cdot t} \left[L(\hat{\mathbf{x}}^{(0)}, \hat{\sigma}^{2(0)}; l_i) - L(\hat{\mathbf{x}}^{(1)}, \hat{\sigma}^{2(1)}; l_i)\right]\right]^2. \qquad \text{Eq. 15}$$

Since the test statistic

Statistical Evaluation of the B-Splines Approximation of 3D Point Clouds (9634)
Hamza Alkhatib, Boris Kargoll, Jens-André Paffenholz and Johannes Bureick (Germany)

FIG Congress 2018
Embracing our smart world where the continents connect: enhancing the geospatial maturity of societies
Istanbul, Turkey, May 6–11, 2018

$$\frac{L(\hat{\mathbf{x}}^{(0)}, \hat{\boldsymbol{\sigma}}^{2(0)}; \mathbf{l}) - L(\hat{\mathbf{x}}^{(1)}, \hat{\boldsymbol{\sigma}}^{2(1)}; \mathbf{l})}{\hat{\boldsymbol{\omega}} \cdot \sqrt{3 \cdot s \cdot \mathrm{t}}} \qquad \text{Eq. 16}$$

follows then approximately (i.e., for large numbers of measurements) the standard normal distribution, the two considered models are significantly different if the statistic takes a value that is less than the $\alpha/2$-quantile or greater than the $1 - \alpha/2$-quantile of $N(0,1)$, where α describes the significance level. The former case indicates that the B-Spline model $\mathbf{A}^{(0)}\mathbf{x}^{(0)}$ is significantly better than the model $\mathbf{A}^{(1)}\mathbf{x}^{(1)}$, the latter case suggests reversely that the model $\mathbf{A}^{(1)}\mathbf{x}^{(1)}$ is significantly closer to the truth than model $\mathbf{A}^{(0)}\mathbf{x}^{(0)}$, and a value between the lower and upper critical value means that the two models are equivalent or practically indistinguishable. It is generally recommended to punish models with great numbers of functional parameters, so that we follow the recommendation of Vuong (1989) and include similar correction terms as in the information criteria. In our case study, we use the BIC-related term to correct the log-likelihoods in the numerator of (16), respectively, to

$$L(\hat{\mathbf{x}}^{(0)}, \hat{\boldsymbol{\sigma}}^{2(0)}; \mathbf{l}) - \frac{1}{2} \cdot (3 \cdot [n^{(0)} + 1] \cdot [l^{(0)} + 1] + 1) \cdot \log(3 \cdot s \cdot \mathrm{t}) \qquad \text{Eq. 17}$$

and

$$L(\hat{\mathbf{x}}^{(1)}, \hat{\boldsymbol{\sigma}}^{2(1)}; \mathbf{l}) - \frac{1}{2} \cdot (3 \cdot [n^{(1)} + 1] \cdot [l^{(1)} + 1] + 1) \cdot \log(3 \cdot s \cdot \mathrm{t}). \qquad \text{Eq. 18}$$

These modifications leave the test distribution asymptotically unchanged.

2.2.2 Clarke's Testing Approach

When comparing different B-Spline models, we essentially vary the design matrix within the observation equations while the remaining structure (i.e., the stochastic model) remains unchanged. As mentioned earlier, different B-Spline designs usually give rise to design matrices that are non-nested. Clarke (2007) noted that in such a situation, the probability distribution of the likelihood ratio statistic (or equivalently of the log-likelihood difference) is often found to be highly peaked in comparison to a Gaussian distribution. To account for this finding, Clarke (2003) proposed a *distribution-free test*, for which the distribution of the test statistic does not depend on the normality of the likelihood ratio. Instead of testing the difference between the likelihoods given the entire data set $\mathbf{l}$ as in (16), the idea now is to compute the differences

$$d_i = L(\hat{\mathbf{x}}^{(0)}, \hat{\boldsymbol{\sigma}}^{2(0)}; l_i) - L(\hat{\mathbf{x}}^{(1)}, \hat{\boldsymbol{\sigma}}^{2(1)}; l_i) \qquad \text{Eq. 19}$$

between the log-likelihoods at each observation l_i individually and to count the total number B of positive differences. In case the competing models are similar, that number is expected to be small. The sum B follows a Binomial distribution (whose parameters are naturally given firstly by the number of observations or compared log-likelihood values $3 \cdot s \cdot \mathrm{t}$ and secondly by the a-priori probability 0.5 of obtaining a positive log-likelihood difference). Thus, the two competing models are significantly different if the statistic B turns out to be less than the $\alpha/2$-quantile or greater than the $1 - \alpha/2$-quantile of that Binomial distribution. In analogy to Vuong's test, we follow the proposal of Clarke (2007) and punish overly large models by correcting the compared log-likelihoods in (18), respectively, to

$$L(\hat{\mathbf{x}}^{(0)}, \hat{\boldsymbol{\sigma}}^{2(0)}; l_i) - \frac{1}{2 \cdot 3 \cdot s \cdot \mathrm{t}} \cdot (3 \cdot [n^{(0)} + 1] \cdot [l^{(0)} + 1] + 1) \cdot \log(3 \cdot s \cdot \mathrm{t}) \qquad \text{Eq. 20}$$

and

Statistical Evaluation of the B-Splines Approximation of 3D Point Clouds (9634)
Hamza Alkhatib, Boris Kargoll, Jens-André Paffenholz and Johannes Bureick (Germany)

FIG Congress 2018
Embracing our smart world where the continents connect: enhancing the geospatial maturity of societies
Istanbul, Turkey, May 6–11, 2018

$$L(\hat{\mathbf{x}}^{(1)}, \hat{\boldsymbol{\sigma}}^{2(1)}; l_i) - \frac{1}{2 \cdot 3 \cdot s \cdot t} \cdot (3 \cdot [n^{(1)} + 1] \cdot [l^{(1)} + 1] + 1) \cdot \log(3 \cdot s \cdot t). \qquad \text{Eq. 21}$$

As for Vuong's test, the distribution of the test statistic can be maintained under these dimensionality correction.

3. CASE STUDY

3.1 Experiment Design and Data Acquisition

The object under investigation in this case study is an historic masonry arch bridge over the river Aller near Verden (Lower Saxony, Germany). The aim of the experiment was the combination of numerical models and experimental investigations for model calibration (Schacht et al., 2016). The project team under the leadership of the Institute of Concrete Construction of the Leibniz Universität Hannover has carried out two load test with a maximum load of 570 t (!) in March and June 2016. The contributions from researchers of the Geodetic community were the detection of load-induced arch displacements by means of, e.g., laser tracker and laser scanner, which is discussed, e.g. in Paffenholz et al. (2018a), Paffenholz et al. (2018b) and Wujanz et al. (2018).

The historic masonry arch bridge was made of circular brick arches of following dimensions: width 14m, depth 8m and height 4-6m. Figure 1 shows the side view from West of the arch 4 under investigation.

In the scope of the load testing the standard load of 1.0 MN (100 t) should be clearly excited. By this setup first nonlinear deformations should be detected. According to Schacht et al. (2016) and the references therein, performed numerical simulations stated that a loading with five-times the standard load has to be realized. Thus, a maximum load of approximately 6.0 MN was defined which will be produced by four hydraulic cylinders. These hydraulic cylinders were mounted on the arch (see Figure 1). The counteracting force was realized by injection piles of length 18 m in depth. The connection of hydraulic cylinders and injection piles is realized by threaded rods. A detailed description of the bridge structure as well as the design of experiments can be found in Schacht et al. (2016) and Schacht et al. (2018).

Statistical Evaluation of the B-Splines Approximation of 3D Point Clouds (9634)
Hamza Alkhatib, Boris Kargoll, Jens-André Paffenholz and Johannes Bureick (Germany)

FIG Congress 2018
Embracing our smart world where the continents connect: enhancing the geospatial maturity of societies
Istanbul, Turkey, May 6–11, 2018

Figure 1: Side view from West of the arch 4 of the historic masonry arch bridge. The whitewashed area indicates the area of the direct influence of the load application. In the foreground: Baseline for the estimation of the vertical deflection at three discrete locations. On the bridge: four hydraulic cylinders for the load application.

The Geodetic Institute Hanover has used the terrestrial laser scanner Zoller+Fröhlich (Z+F) Imager 5006 to capture 3D point clouds of the entire underside of the arch. The data acquisition was carried out in periods of a constant load on the bridge. Details of the loading regime can be found in Paffenholz et al. (2018a). The setup of the laser scanner was carefully chosen outside the danger zone in case of a structural collapse and under consideration of an almost optimal object distance and angle of impact of the laser beam on the surface of the arch. Since in this contribution, the focus is on the approximation of 3D point clouds by means of B-Splines, we have chosen the reference epoch of load 100 kN to statistical investigate our different approximation approaches. For an in-depth discussion of the experiment and results for vertical displacements is referred to Paffenholz et al. (2018a) and Wujanz et al. (2018).

3.2 Preparation of Data Sets

For the approximation of the 3D point clouds by means of B-Spline surface some preparatory steps have to be performed. Firstly, interfering objects which most likely appear differently in various load steps should be carefully removed from the 3D point clouds. These interfering objects are for instance other sensor installations like prisms for the laser tracker and strain gauges. Previous investigations have shown, that aforementioned objects appear differently in the load steps and thus could lead to misinterpretations in the subtraction of a load step with respect to a reference epoch. Secondly, a buffering is performed to reduce the 3D point cloud in the margin areas with the aim to handle data gaps in the margin areas and improve the B-Spline approximation. Thirdly and lastly, an initial approximation by means of a projection of the 3D point cloud on a regular grid is performed. These simple gridding approach is justified due to a homogenous curvature of the arch which is characterized by non-occuring curvature changes. Sophisticated approaches to deal with complex surfaces, like Coons Patches, are discussed by Harmening & Neuner (2015). The grid size is chosen with respect to the dimensions of the 3D point cloud of the arch. Chosen is a size of 9 m, i.e. 400 grid cells, perpendicular to the bridge centerline and 14 m, i.e. 600 grid cells, in direction of the bridge centerline. This gridding results in nearly quadratic grid cells of size 2.2 cm and each cell holds 10 3D points of the 3D point cloud.

4. RESULTS OF THE INVESTIGATION

In order to select the proper B-Spline model as a representation of the optimal modeled surface, the number of control points (resulting into the total number of parameters) as well as the optimal knot vector should be determined. For this reason we evaluate B-Spline surface models described in Section 2.1 with increasing the control points in $\bar{u}$- and $\bar{v}$-direction from 5 to 41. We obtained in total 1369 combinations.

Statistical Evaluation of the B-Splines Approximation of 3D Point Clouds (9634)
Hamza Alkhatib, Boris Kargoll, Jens-André Paffenholz and Johannes Bureick (Germany)

FIG Congress 2018
Embracing our smart world where the continents connect: enhancing the geospatial maturity of societies
Istanbul, Turkey, May 6–11, 2018

4.1 AIC and BIC information criteria
4.2

First the well-known penalization information criteria (AIC and BIC) are calculated (see. Eq. 11 and 12). The resulting numbers are sorted according to the amount of model parameter from the smallest to the largest number of parameters. The result is shown in Figure 2 for different knot vector determination techniques. We see clearly that our knot vector determination approach MCM (Bureick et al., 2016) leads in all models to smaller AIC and BIC than the standard approach KPT introduced in Piegl & Tiller (1997). We use AIC and BIC in order to discriminate between B-Spline surface models. The minimum values for both criteria numbers and both knot vector determination are summarized in Table 1.

Table 1: Minimum number of AIC and BIC.

|	KPT		MCM	
	n	*l*	*n*	*l*
AIC	39	27	37	27
BIC	12	9	15	8
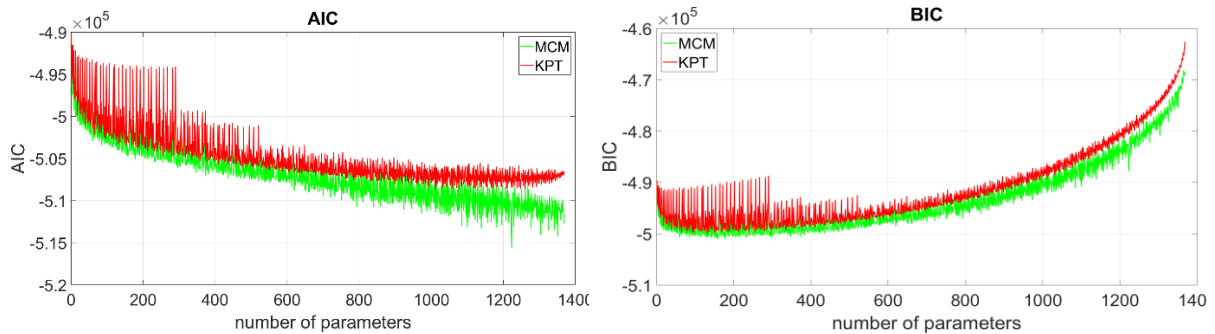
Figure 2: Results for AIC (left) and BIC (right) for two different knot vector determination approaches: Evolutionary Monte Carlo Method (MCM) developed by Bureick et al. (2016) and knot placement technique (KPT) described in Piegl & Tiller (1997).

4.3 Evaluation of competing B-Spline models with Voung and Clarke testing approaches

In order to select the best B-Spline surface model from the 1369 possible combinations for every knot vector determination approach, we use the model selection approaches based on Voung's and Clarke's test described in Section 2.2.1 and 2.2.2 respectively. The best model should fulfill the balance between model complexity and proper approximation quality. For this reason every model from the 1369 possible combinations should be tested against the other 1368 combinations, which results in about 2 million implementations of the both test approaches for every knot vector determination method, which lead to enormous time and computing capacity. Thus we developed a test strategy which needs much less combinations. First we search for every model $M(n, l)$ all neighbouring models $M_{nei}(n_{nei}, l_{nei})$ which fulfil the following conditions: $n - c \leq n_{nei} \leq n + c$ and $l - c \leq l_{nei} \leq l + c$. The constant c gives the maximum neighbouring step for competing models. Afterwards the model $M(n, l)$ (model

Statistical Evaluation of the B-Splines Approximation of 3D Point Clouds (9634)
Hamza Alkhatib, Boris Kargoll, Jens-André Paffenholz and Johannes Bureick (Germany)

FIG Congress 2018
Embracing our smart world where the continents connect: enhancing the geospatial maturity of societies
Istanbul, Turkey, May 6–11, 2018

I) will be tested against all other competing models (model II) lying in the neighbouring area. All competing models, which fulfil following conditions: $n - c < n_{min}$, $n + c > n_{max}$, $l - c < l_{min}$ and $l + c > l_{max}$, will be compared in a further step with model I. In this paper we fixed the constant c to 5 resulting in 120 test implementations at maximum. The models, which are located at the edge, have 35 test implantation at minimum. For every model a scoring is allocated. The scoring of model $M(n, l)$ is increased by the value 1 if this model is tested to be preferred over model II. Otherwise the scoring will be decreased with the value -1. If it is not possible to discriminate between model I and II the scoring will not be changed. After the performing of all possible tests the scoring for the model $M(n, l)$ is divided by the total number of test implementations. Thus a range of values between -1 and 1 is obtained for every model. The value 1 means that model I is better than all neighboring models, and - 1 means, in contrast, that model I is more unreliable than all other neighboring models. Afterwards we select the model with the highest scoring and test it with all other models. If the test result is positive (the model 1 is preferred over all models), then we select this model to be the best model among possible combinations. If this is not the case we select the model, which is better and have then to repeat the same procedure and test this model against all other alternative B-Spline models until we identify a model which is preferred over all other models (1368 possible models). In total the computing effort has been reduced from 2 million to about 150.000 test implementations.

The results for Voung's test approach are depicted in Figure 3. According to Figure 3 the highest obtained scoring in case of applying Voung's test approach has been reached for $M(15,8)$ (rectangle with red edges) using MCM knot determination technique and $M(18,9)$ using KPT technique, respectively. Afterwards we tested the selected model with maximum scoring using Voung's approach against other models. This model was preferred over all other models expect the models depicted in rectangle with magenta edges.
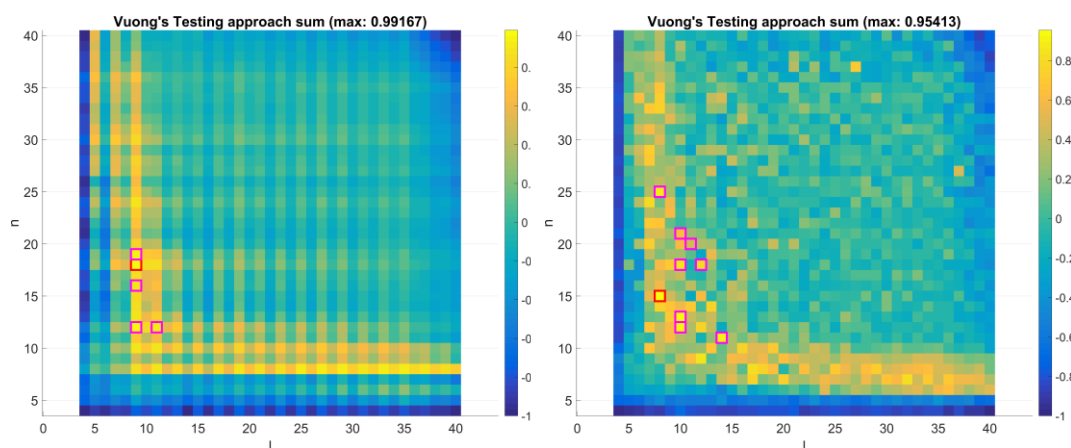
Figure 3: Results for Voung's test for two different knot vector determination: MCM and KPT techniques
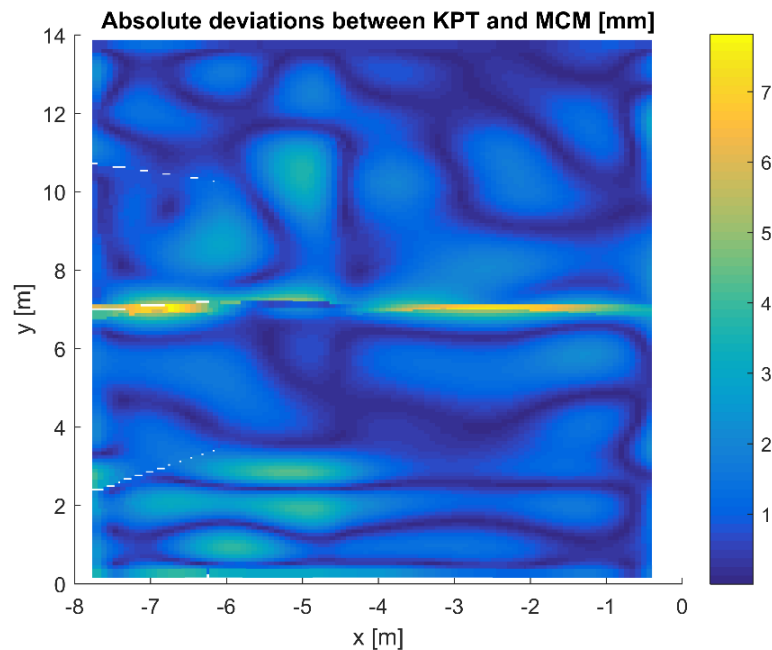
According to Figure 4 the highest obtained scoring in case of applying Clarke's test approach has been reached for $M(15,8)$ (rectangle with red edges) using MCM knot determination

Statistical Evaluation of the B-Splines Approximation of 3D Point Clouds (9634)
Hamza Alkhatib, Boris Kargoll, Jens-André Paffenholz and Johannes Bureick (Germany)

FIG Congress 2018
Embracing our smart world where the continents connect: enhancing the geospatial maturity of societies
Istanbul, Turkey, May 6–11, 2018

technique and $M(12,9)$ using KPT technique, respectively. Afterwards we tested the selected model with maximum scoring using Clarke's approach against other models. This model was preferred over all other models without exception.
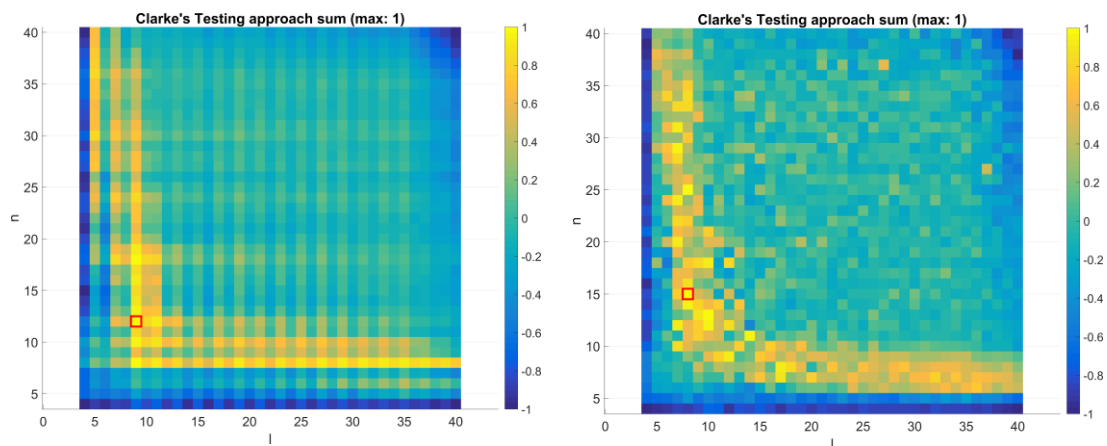
Figure 4: Results for Clarke's test for two different knot vector determination: MCM and KPT techniques

We conclude that Voung's testing approach was not able to identify a unique best model for both knot vector determination techniques. In contrast, the Clarke's testing approach can identify one model to be preferred over all other B-Spline models using two different knot vector determination approaches. If we test both best models from the different knot vector determination techniques using the Clarke's testing approach, the model $M(15,8)$ resulting from MCM technique is preferred over the model $M(12,9)$ resulting from KPT technique with a significance level α of 5%. The absolute deviations of the adjusted observations between both models are displayed in Figure 5.

Statistical Evaluation of the B-Splines Approximation of 3D Point Clouds (9634)
Hamza Alkhatib, Boris Kargoll, Jens-André Paffenholz and Johannes Bureick (Germany)

FIG Congress 2018
Embracing our smart world where the continents connect: enhancing the geospatial maturity of societies
Istanbul, Turkey, May 6–11, 2018

Figure 5: Absolute deviations of the adjusted observations between MCM and KPT

As we can see the absolute deviations between both models are 8 mm at maximum. The largest deviations are centered in the arch crown ($y \approx 7\ m$).

5. CONCLUSION

We show in this paper the Vuong and Clarke tests, which are likelihood-ratio-based tests for model selection that use the Kullback-Leibler information criterion. The implemented tests can be used for choosing between two competing bivariate B-Spline models which are non-nested. In both tests, the null hypothesis is that the two B-Spline models are equivalent, whereas the alternative is that one of both models is better than the other. The Voung test follows asymptotically a standard normal distribution under the null hypothesis whereas the Clarke test follows asymptotically a binomial distribution with two parameters: number of observations and 0.5. For our test study, the Voung test does not perform well and was not able to identify the best B-Spline model. The Clarke's test approach, in contrast, can successfully prefer one model over all other competing models. An identical result is obtained by comparing Clarke's test decision with the widely-used BIC information criterion in discriminating B-Spline surface models. The main difference between Kullback-Leibler information criterion and parametric Voung's and non-parameteric Clarke test is that hypothesis tests make assessment in a framework of likelihood ratio hypothesis testing, which can select the significant probabilistic differences between competing models.

Statistical Evaluation of the B-Splines Approximation of 3D Point Clouds (9634)
Hamza Alkhatib, Boris Kargoll, Jens-André Paffenholz and Johannes Bureick (Germany)

FIG Congress 2018
Embracing our smart world where the continents connect: enhancing the geospatial maturity of societies
Istanbul, Turkey, May 6–11, 2018

REFERENCES

Bureick, J., Alkhatib, H., Neumann, I. (2016): Robust Spatial Approximation of Laser Scanner Point Clouds by Means of Free-form Curve Approaches in Deformation Analysis. Journal of Applied Geodesy 10 (1), pp. 27-35.

Bureick, J.; Alkhatib, H. (2018): Fast converging elitist genetic algorithm for optimal knot adjustment in B-spline curve approximation. Applied Soft Computing. (Under review).

Burnham, K.P., Anderson, D.A. (2002): Model selection and multimodel inference. Second edition, Springer, New York.

Clarke, K.A. (2007): A simple distribution-free test for nonnested model selection. Political Analysis 15, pp. 347-363.

Clarke, K.A. (2003): Nonparametric model discrimination in international relations. Journal of Conflict Resolution 47 (1), pp. 72-93.

Cox, M.G. (1972): The Numerical Evaluation of B -Splines. IMA J Appl Math 10 (2), pp. 134-149.

de Boor, C. (1972): On calculating with B-splines. Journal of Approximation Theory 6 (1), pp. 50-62.

Dierckx, P. (1993). Curve and surface fitting with splines. Clarendon Press, Oxford [i.a.], XVII, 285 p.

Gálvez, A., Iglesias, A., Avila, A., Otero, C., Arias, R., Manchado, C. (2015): Elitist clonal selection algorithm for optimal choice of free knots in B-spline data fitting. Applied Soft Computing 26, pp. 90-106.

Harmening, C., Neuner, H.B. (2015): A constraint-based parameterization technique for B-spline surfaces. Journal of Applied Geodesy 9 (3). pp. 143-161.

Harmening, C., Neuner, H.B. (2016): Choosing the optimal number of B-spline control points (Part 1: Methodology and approximation of curves). Journal of Applied Geodesy 10 (3), pp. 139-157.

Harmening, C., Neuner, H.B. (2017): Choosing the optimal number of B-spline control points (Part 2: Approximation of surfaces and applications). Journal of Applied Geodesy 11 (1), pp. 43-52.

Koch, K. R. (2009): Fitting free-form surfaces to laserscan data by NURBS, AllgemeineVermessungs-Nachrichten (AVN) 116 (4) (2009) 134–140.

Koch, K.R. (1999): Parameter estimation and hypothesis testing in linear models. Springer,

Lehmann, R., Lösler, M. (2017): Congruence analysis of geodetic networks - hypothesis tests versus model selection by information criteria. Journal of Applied Geodesy 11 (4), pp. 271-283.

Ma, W., Kruth, J.P. (1995): Parameterization of randomly measured points for least squares fitting of B-spline curves and surfaces. Computer-Aided Design 27 (9), pp. 663-675.

Paffenholz, J.-A.; Huge, J.; Stenz, U. (2018a): Integration von Lasertracking und Laserscanning zur optimalen Bestimmung von lastinduzierten Gewölbeverformungen. In: allgemeine vermessungs-nachrichten (avn), 125. Jg., to appear.

Statistical Evaluation of the B-Splines Approximation of 3D Point Clouds (9634)
Hamza Alkhatib, Boris Kargoll, Jens-André Paffenholz and Johannes Bureick (Germany)

FIG Congress 2018
Embracing our smart world where the continents connect: enhancing the geospatial maturity of societies
Istanbul, Turkey, May 6–11, 2018

Paffenholz, J.-A.; Stenz, U.; Neumann, I.; Dikhoff, I.; Riedel, B. (2018b): Belastungsversuche an einer Mauerwerksbrücke: Lasertracking und GBSAR zur Verformungsmessung. In Mauerwerk-Kalender 2018; Jäger, W., Ed.: Ernst & Sohn: Berlin.

Piegl, L.A., Tiller, W. (1997): The NURBS book, 2nd ed. Springer, Berlin, New York, xiv, 646.

Schacht, G.; Piehler, J.; Marx, S.; Müller, J. Z. (2016): Belastungsversuche an einer historischen Eisenbahn-Gewölbebrücke. In: Bautechnik 94(2016)2, 125 - 130. DOI: 10.1002/bate.201600084.

Schacht, G.; Müller, L.; Piehler, J.; Meichsner, E.; Marx, S. (2018): Belastungsversuche an einer Mauerwerksbrücke: Planung und Vorbereitung der experimentellen Untersuchungen. In Mauerwerk-Kalender 2018; Jäger, W., Ed.: Ernst & Sohn: Berlin.

Vuong, Q.H. (1989): Likelihood ratio tests for model selection and non-nested hypotheses. Econometrica 57 (2), pp. 307-333.

Wujanz, D.; Burger, M.; Neitzel, F.; Lichtenberger, R.; Schill, F.; Eichhorn, A.; Stenz, U.; Neumann, I.; Paffenholz, J.-A. (2018): Belastungsversuche an einer Mauerwerksbrücke: Terrestrisches Laserscanning zur Verformungsmessung. In Mauerwerk-Kalender 2018; Jäger, W., Ed.: Ernst & Sohn: Berlin.

Zhao, X., Kargoll, B., Omidalizarandi, M., Xu, X.,Alkhatib, H. (2018): Model selection for parametric surfaces approximation 3D point clouds for deformation analysis. Remote Sensing. (Under review).

BIOGRAPHICAL NOTES

Dr.-Ing. Hamza Alkhatib received his diploma (Dipl.-Ing.) in Geodesy at the Karlsruhe Institute of Technology (KIT) in 2001 and his doctorate (Dr.-Ing.) at the Faculty of Agriculture of the University of Bonn in 2007. Since 2007 he has been postdoctoral fellow at the Geodetic Institute at the Leibniz Universität of Hannover. His main research interests are: Bayesian statistics, Monte Carlo simulation, modeling of measurement uncertainty, filtering and prediction in state space models, and gravity field recovery via satellite geodesy.

Dr.-Ing. Boris Kargoll received his diploma (Dipl.-Ing.) in Geodesy at the Karlsruhe Institute of Technology (KIT) in 2001 and his doctorate (Dr.-Ing.) at the Faculty of Agriculture of the University of Bonn in 2007. Between 2001 and 2016, he was a scientific employee at the Theoretical Geodesy Group of the Institute of Geodesy and Geoinformation in Bonn. Since 2016, he has been a scientific employee in the Engineering Geodesy and Geodetic Data Analysis department at the Geodetic Institute of the Leibniz Universität Hannover. His main research interests are in the fields of (self-tuning) robust parameter estimation, stochastic processes, and model testing.

Johannes Bureick received his Master of Science in Geodesy and Geoinformatics at the Leibniz Universität Hannover in 2011. He passed the highest-level state certification as "Graduate Civil Servant for Surveying" in North Rhine-Westphalia in 2013. Since 2013 he is working at the Geodetic Institute at the Leibniz Universität Hannover. His research focus is on B-Spline approximation and the development of Multi-Sensor-Systems.

Statistical Evaluation of the B-Splines Approximation of 3D Point Clouds (9634)
Hamza Alkhatib, Boris Kargoll, Jens-André Paffenholz and Johannes Bureick (Germany)

FIG Congress 2018
Embracing our smart world where the continents connect: enhancing the geospatial maturity of societies
Istanbul, Turkey, May 6–11, 2018

Dr.-Ing. Jens-André Paffenholz received his diploma (Dipl.-Ing.) and his Ph.D. in Geodesy and Geoinformatics at the Leibniz Universität Hannover in 2006 and 2012, respectively. Since 2014, he has been postdoctoral fellow and the leader of the working group Terrestrial Laser Scanner Based Multi-Sensor Systems | Engineering Geodesy at the Geodetic Institute of the Leibniz Universität Hannover. His research profile is based on laser scanning and multi-sensor systems with the aim of an efficient three-dimensional data acquisition for monitoring and change detection of natural and anthropogenic structures. He is active in national (DVW e. V. WG 4: "Engineering Surveys") and international scientific associations (working group chair of IAG WG 4.1.3: "3D Point Cloud based Spatio-temporal Monitoring"). ORCID ID: https://orcid.org/0000-0003-1222-5568

CONTACTS

Dr.-Ing. Hamza Alkhatib Geodetic Institute Leibniz Universität Hannover Nienburger Str. 1, 30167 Hannover GERMANY Phone: +49 (0) 511-762 2464 E-mail: alkhatib@gih.uni-hannover.de Web page : www.gih.uni-hannover.de	Dr.-Ing. Boris Kargoll Geodetic Institute Leibniz Universität Hannover Nienburger Str. 1, 30167 Hannover GERMANY Phone: +49 (0) 511-762 3585 E-mail: kargoll@gih.uni-hannover.de Web page : www.gih.uni-hannover.de
Johannes Bureick, M.Sc. Geodetic Institute Leibniz Universität Hannover Nienburger Str. 1, 30167 Hannover GERMANY Phone: +49 (0) 511-762 5190 E-mail: bureick@gih.uni-hannover.de Web page : www.gih.uni-hannover.de	Dr.-Ing. Jens-André Paffenholz Geodetic Institute Leibniz Universität Hannover Nienburger Str. 1, 30167 Hannover GERMANY Phone: +49 (0) 511-762 3191 E-mail: paffenholz@gih.uni-hannover.de Web page : www.gih.uni-hannover.de

Statistical Evaluation of the B-Splines Approximation of 3D Point Clouds (9634)
Hamza Alkhatib, Boris Kargoll, Jens-André Paffenholz and Johannes Bureick (Germany)

FIG Congress 2018
Embracing our smart world where the continents connect: enhancing the geospatial maturity of societies
Istanbul, Turkey, May 6–11, 2018